Ion Recognition at the Interface of Self-Assembled Monolayers (SAMs) of Bis-Thioctic Ester Derivatives of Oligo(ethyleneglycols)

Krisanu Bandyopadhyay, Sheng-Gao Liu, Haiying Liu, and Luis Echegoyen*[a]

Abstract: Self-assembled monolayers (SAMs) of bis-thioctic ester derivatives of oligoethylene glycols were prepared. When the number of $(-CH_2-CH_2-O-)_n$ units in these podands was either five or six, the corresponding SAMs showed ion binding properties and selectivities similar to those exhibited by 15-crown-5 or 18-crown-6 in aqueous solution, respectively. Impedance data for the SAMs as a function of metal ion concentrations were fitted by using a Langmuir isotherm to determine the association constants (K_a) with the different ions. The SAM derived from the $n=5$ compound is selective for Na^+ while that with $n=6$ is selective for K^+. Results presented here confirm the formation of ion recognition domains during self-assembly of acyclic polyethylene glycol derivatives on gold surfaces; this suggests that surface-confined *pseudocrown ether* structures are formed.

Keywords: crown compounds · impedance spectroscopy · monolayers · polyethylene glycol · supramolecular chemistry

Introduction

Self-assembled monolayer (SAM) formation is an effective technique to modify surfaces in order to obtain a desired property.[1] SAM structures with specific terminal functionalities have been prepared for the recognition and sensing of metal ions, some of which are electrochemically active, while others are not.[2] Cyclic voltammetry and impedance spectroscopy have been used successfully for the detection of the ion binding events on the monolayer-modified surfaces.[2, 3] Detection of electrochemically active metal ions is typically done following their direct voltammetric responses,[2] while electrochemically inactive cations can be detected indirectly following the changes in the monolayer capacitance and/or resistance.[3] Alternatively, if the SAM itself contains an electroactive center that responds to the ion binding event directly, it can be used to monitor binding with electrochemically inactive ions.[4, 5]

The incorporation of crown-ether groups into SAM structures and their potential as metal ion sensors were reported recently by Flink et al.[6] and Moore et al.[4] In one report, monolayers were formed from 12-crown-4, 15-crown-5, or 18-crown-6 derivatives with single alkyl chain thiols, and the ion binding events were monitored by using impedance spectroscopy.[6] The other work concerned a crown-annelated tetrathiafulvalene (TTF) derivative, which showed a direct response of the electroactive surface-confined crown-TTF group due to ion complexation.[4] We have also recently prepared and studied bis-thioctic ester derivatives of crown ether annelated TTFs, which form remarkably stable SAMs; some of these were also able to detect alkali metal ion binding by means of electrochemical measurements.[5]

In all of the cases mentioned above, a crown-ether ring structure was present as a terminal group in the monolayer to bind ions directly at the solution interface. SAMs and mixed SAMs with acyclic polyethylene glycol (PEG) as hydrophilic spacers have been studied mainly for supported bilayer construction and to create surfaces to repel proteins and cells, not as ion recognition motifs.[7] To our knowledge, ion recognition and sensing abilities by PEG-containing monolayers had not been explored at all, except recently, when we reported that SAMs of bis-thioctic ester derivatives of oligoethylene glycol (podands) are capable of forming selective ion binding domains on surfaces by means of self-assembly.[8]

In this paper, we provide further evidence of ion recognition of SAMs derived from other acyclic polyethers: *bis*-thioctic ester podands with $(-CH_2-CH_2-O-)_5$ units. Moreover, comparison of the earlier published results[8] with those for a monolayer of a thioctic ester derivative of 18-crown-6 proves that the acyclic podands form surface-assisted pseudocrown ether structures during self-assembly at the interface. The monolayer derived from the $(-CH_2-CH_2-O-)_6$ containing podand is selective for K^+, and that derived from $(-CH_2-CH_2-O-)_5$ is selective for Na^+. The selectivity is higher for the surface-confined podands compared with that observed for the macrocyclic crown structures in monolayers and in solution.

[a] Prof. L. Echegoyen, Dr. K. Bandyopadhyay, Dr. S.-G. Liu, Dr. H. Liu
Department of Chemistry, University of Miami
Coral Gables, FL 33124-0431 (USA)
Fax: (+1) 305-284-4571
E-mail: echegoyen@miami.edu

  0947-6539/00/0623-4385 $ 17.50+.50/0

Results and Discussion

Monolayer characterization: Reflection absorption infrared spectroscopy (RAIRS) can effectively be used to analyze monolayer formation and the degree of organization. In the present case, all monolayers were characterized by RAIRS, and the essential features of the spectra are similar for all compounds studied, since they are structurally similar. The main peak assignments are given in Table 1. In the higher frequency region, there are two absorption bands due to methylene stretching vibrations from both alkyl and oligoethylene glycol (OEG) units of **1** and **2**, and from the crown ether moiety of **3**. The peak positions of the respective methylene vibration bands in the monolayer are almost the same when compared with the transmission spectra of the compounds; this indicates that the alkyl chains in all of the monolayers are in a liquidlike disordered state.[9] Analysis of the spectra in the lower frequency region shows a strong absorption band in the region of 1740 to 1721 cm^{-1} for the −C−O stretching of the carbonyl group.[10] Furthermore, a strong absorption band is observed at 1129 cm^{-1} for the monolayer of compound **1** and at 1126 cm^{-1} for that of **2**, attributed to the parallel polarized −C−O−C− stretching mode of the OEG part of the monolayer.[11] Moreover, there are shoulders in the lower frequency region of the −C−O−C− stretching band at 1118 cm^{-1} for **1** and 1121 cm^{-1} for **2**; these correspond to the −C−O−C− stretching mode perpendicular to the OEG helical axis.[12] On the other hand, only a sharp peak was observed at 1138 cm^{-1} for **3**, and this is characteristic of the C−O stretching mode of the ether group.[13]

Table 1. Vibrational mode assignment [cm^{-1}] of major peaks from RAIR spectroscopy of different monolayers on a gold surface.

SAM of **1**	SAM of **2**	SAM of **3**	Assignment
2925	2925	2924	ν_{as} (CH_2) alkyl unit
2868	2857	2852	ν_s (CH_2) OEG unit
1721	1733	1728	ν (−C=O)
1449	1454	1454	CH_2 deformation
1126	1129		ν (C−O−C)
1118	1121		ν (C−O−C)
		1138	ν (−C−O) ether group
1036	1044	1036	CH_2 rocking
948	948	949	

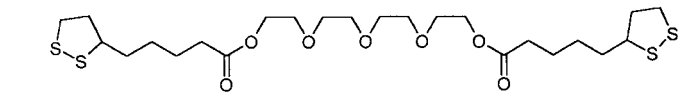

1

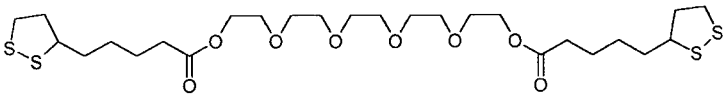

2

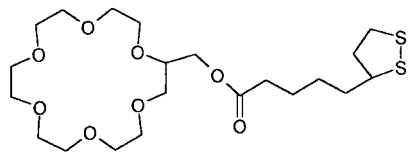

3

Reductive desorption of the monolayer in KOH (0.5 M) was used to estimate the surface coverage.[14] In all three cases, an irreversible cathodic wave was observed at about −0.9 V versus Ag/AgCl, which corresponds to the surface-attached thiolate groups. Integration of the current under the cathodic wave, and normalizing the results on the basis of the number of sulfurs presumably bonded to the surface (four in the case of **1** and **2**, and two for **3**) provide an estimated surface coverage of 3.3×10^{-11}, 6.2×10^{-11}, or 4.6×10^{-11} for **1**, **2**, and **3**, respectively. These values are lower than that observed for a thioctic acid[15] (which is the anchoring segment for all the compounds) monolayer on gold. The reduced surface coverage is partly due to the larger size and the presence of the two disulfide functionalities in **1** and **2** and is also caused by the presence of a terminal crown ether group in **3**. It also probably reflects the formation of less densely packed monolayers, due to the inherent disorder of the podands and the lack of mobility of the surface-confined disulfide groups. It was observed that monolayers of **1** and **2** desorb at a more cathodic potential than for **3** (order: **2** > **1** > **3**; −1.03 V, −0.99 V, and −0.95 V versus Ag/AgCl), which suggests a stability order for these monolayers and reflects the increased number of surface-attached sulfur groups in **1** and **2**.[16]

Double-layer capacitance was also estimated for all of these monolayers in Et_4NCl (0.1 M) by cyclic voltammetry (CV) as well as by impedance techniques to assess the quality of the monolayer. The values are 16.4, 11.2, and 13.3 $\mu F\,cm^{-2}$ for monolayers of **1**, **2**, and **3**, respectively; these values can be compared with 25 $\mu F\,cm^{-2}$ for bare gold electrodes and 8.5 $\mu F\,cm^{-2}$ for a thioctic acid monolayer on Au in KCl solution (0.1 M).[17] The higher value of the capacitance relative to that of thioctic acid is due to the higher oxygen content of the monolayers, which increases the dielectric constant. These results also suggest that these monolayers are not densely packed, and that ions in solution can easily permeate through them.

Another way to check the packing density of the monolayers is by investigating their blocking effects on the voltammetric behavior of electroactive species in solution. For a monolayer of fixed thickness, the degree of electrode blocking increases as the density of defects decreases. CVs of $[Ru(NH_3)_6]^{3+}/[Ru(NH_3)_6]^{2+}$ (1 mM) in Et_4NCl (0.1 M) for all three monolayer-modified gold electrodes hardly show any influence on the heterogeneous electron transfer processes of the solution probe. Peak currents and peak to peak separations for the couple at $E^0_{1/2} = -0.2$ V versus Ag/AgCl remain essentially constant for monolayers of **1**, **2**, and **3** when compared with the values observed for bare gold electrodes. Thus the films are permeable to the redox-active species. While this may sound undesirable from a simple packing density perspective, it may be optimal for ion sensing, in which accessibility and binding are crucial (see below). Impedance measurements also support these conclusions since no well-

0947-6539/00/0623-4386 $ 17.50+.50/0 *Chem. Eur. J.* **2000**, *6*, No. 23

defined high frequency semicircle was present in the complex plane impedance plot for all three monolayers in the same electrolyte solution. However, the monolayer derived from compound **2** shows a better blocking ability (from CV) as well as a higher charge-transfer resistance value (R_{ct}, from impedance) compared with the monolayers of **1** and **3**; this is in agreement with the surface coverages as well as with the double-layer capacitance measurements (see Table 2).

Monolayers from compound **4** and **5** were also studied to see the effect of oxygen removal from the podand and

Table 2. Parameters obtained from different electrochemical measurements for respective monolayers on a gold surface.

	SAM of **1**	SAM of **2**	SAM of **3**	SAM of thioctic acid
capacitance [$\mu F\,cm^{-2}$]	16.4	11.2	13.3	8.5
surface coverage [$mol\,cm^{-2}$]	3.3×10^{-11}	6.2×10^{-11}	4.6×10^{-11}	3.1×10^{-10}

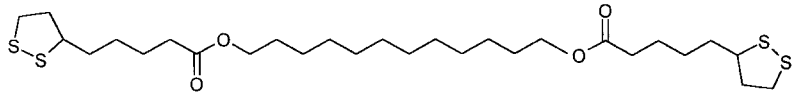

4

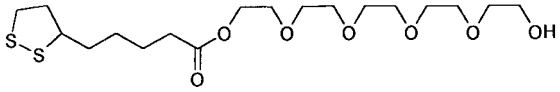

5

removal of one thioctic ester group on ion binding. Figures 1a and b show the impedance response of monolayers **4** and **5**, respectively. It is evident that monolayers of **4** provide effective blocking of charge transfer to the redox probe in solution ($R_{ct} = 70\ k\Omega$), but this is not the case with **5**.

Ion binding properties of the monolayers: Impedance spectroscopy is an effective tool to understand interfacial ion recognition phenomena when both the guest ion and the host monolayer are electrochemically inactive.[3, 5] Double-layer capacitance (C_{dl}) and charge-transfer resistance (R_{ct}) can be used to follow the ion binding processes at the monolayer/solution interface. R_{ct} of the monolayer in the presence of a redox species like $[Ru(NH_3)_6]^{3+}/[Ru(NH_3)_6]^{2+}$ in solution is drastically affected by changes in the surface charge that arise from the incorporation of cationic charge in the monolayer.

Figure 2a shows the complex plane impedance response of a monolayer of **1** in aqueous Et_4NCl solution (0.1M) with $[Ru(NH_3)_6]^{3+}/[Ru(NH_3)_6]^{2+}$ upon addition of increased $[Na^+]$. Essentially no semicircle is observed at the higher frequencies for the monolayer in the absence of Na^+, and a pronounced diffusional component is observed at the lower frequencies; this indicates inefficient blocking of charge transfer. Addition of Na^+ to the solution increases the R_{ct} values, from 3.7 $k\Omega$ at 5mM to a limiting value of 19.4 $k\Omega$ for 45mM of $[Na^+]$; this is similar to the recently reported behavior for a monolayer of **2** with $[K^+]$.[8] This process is perfectly reversible. Interestingly no appreciable increase in the R_{ct} was observed upon addition of K^+. Figure 2b shows a comparison of the impedance response of a monolayer of **1** in both solutions of $[Na^+]$ and $[K^+]$ (45mM). The fitting of all the impedance responses was done by using the program EQUIVALENT CIRCUIT, which determines the circuit parameters by a nonlinear least-square fit to an appropriate equivalent circuit.[8] The R_{ct} obtained for 45mM $[K^+]$ is almost equal to that obtained for the monolayer alone. On the other hand, a $\approx$450% increase from the initial R_{ct} of the monolayer was detected in 45mM of $[Na^+]$. This ion response selectivity can easily be observed from the plots of ΔR_{ct} versus concentration for these ions as shown in Figure 3. Interestingly, a sigmoidal curve is observed for $[Na^+]$ while the R_{ct} value remains almost constant for $[K^+]$. As previously mentioned and reported, a monolayer of **2** binds K^+ selectively over Na^+.[8]

For comparison, a monolayer derived from compound **3**, which has an 18-crown-6 terminal group and a thioctic acid residue as the anchoring segment, was studied. Figure 4 shows the impedance response of the monolayer of **3** and the effect of increasing the concentration of $[K^+]$ in the presence of $[Ru(NH_3)_6]^{3+}/[Ru(NH_3)_6]^{2+}$ as the redox probe in solution.

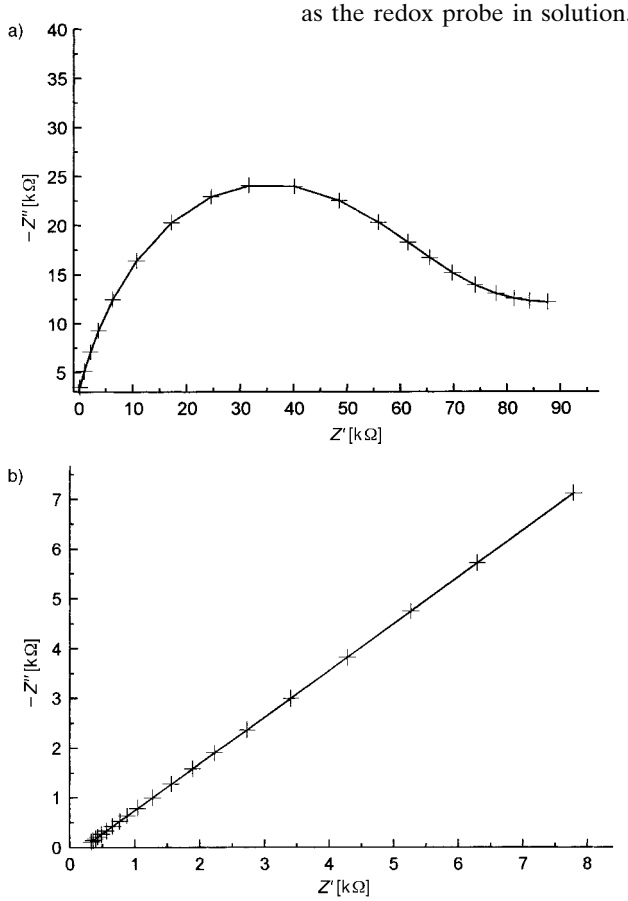

Figure 1. Complex impedance plot at dc bias of -0.20 V versus Ag/AgCl in $[Ru(NH_3)_6]^{3+}/[Ru(NH_3)_6]^{2+}$ (1mM) + aqueous solution of tetraethylammonium chloride (0.1M) for a) monolayer **4** and b) **5**. The frequency range used was 1 kHz to 0.1 Hz with a 5 mV rms signal at ten steps per decade. Solid lines are the fit to the experimental response by using the appropriate equivalent circuit (see text).

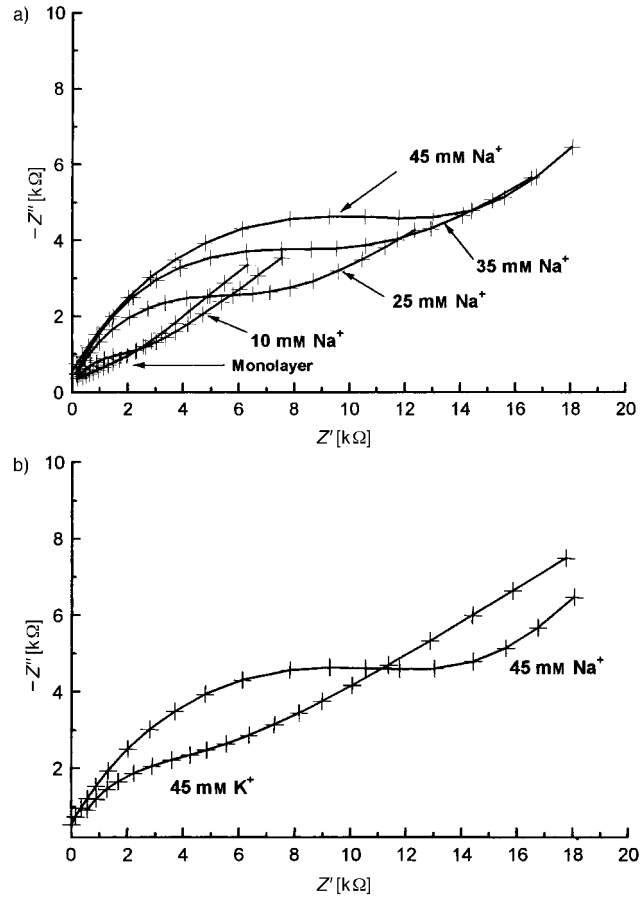

Figure 2. a) Complex impedance plot at dc bias of -0.20 V versus Ag/AgCl in $[Ru(NH_3)_6]^{3+}/[Ru(NH_3)_6]^{2+}$ (1 mM) + aqueous solution of tetraethylammonium chloride (0.1M) for the monolayer **1** in the presence of an increased concentration of $[Na^+]$. b) Comparative complex impedance plot at dc bias of -0.20 V versus Ag/AgCl in $[Ru(NH_3)_6]^{3+}/[Ru(NH_3)_6]^{2+}$ (1 mM) in an aqueous solution of tetraethylammonium chloride (0.1M) for the monolayer **1** in the presence of $[Na^+]$ and $[K^+]$ (45 mM). The frequency range used was 1 kHz to 0.1 Hz with a 5 mV rms signal at ten steps per decade. Solid lines are the fit to the experimental response by using the appropriate equivalent circuit (see text).

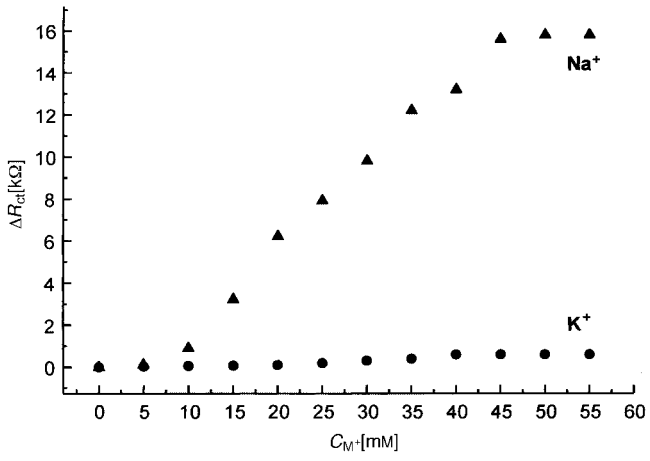

Figure 3. Plot of ΔR_{ct} versus concentration of $[Na^+]$ and $[K^+]$ for the monolayer of **1**.

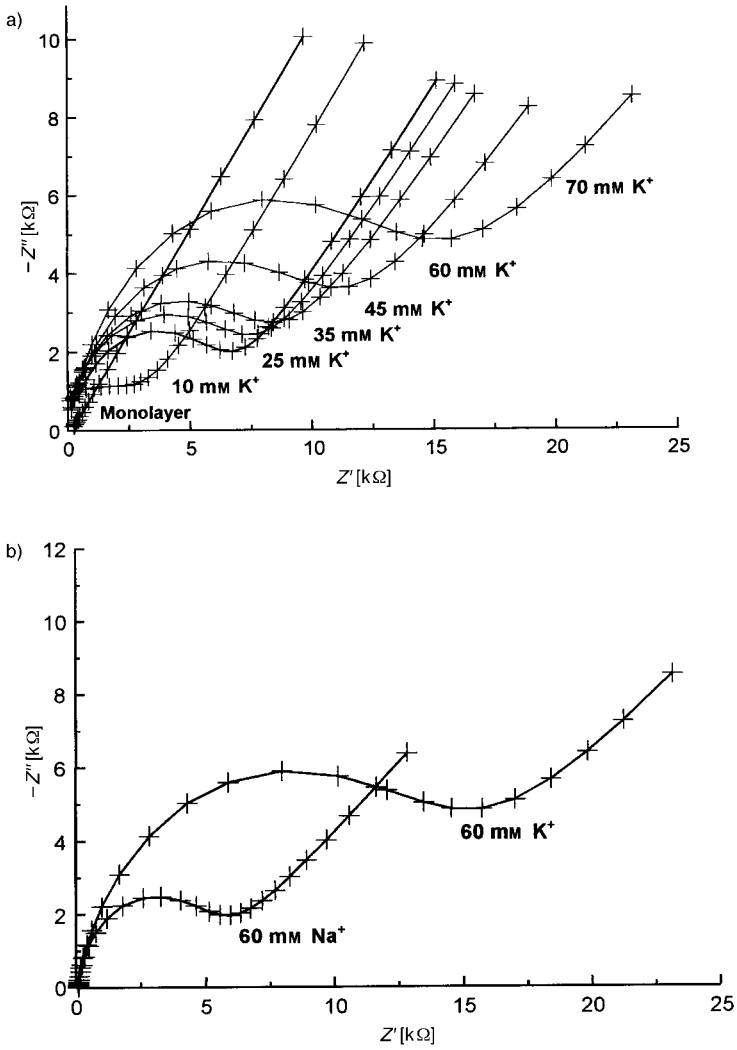

Figure 4. a) Complex impedance plot at dc bias of -0.20 V versus Ag/AgCl in $[Ru(NH_3)_6]^{3+}/[Ru(NH_3)_6]^{2+}$ (1 mM) in an aqueous solution of tetraethylammonium chloride (0.1M) for the monolayer **3** in the presence of an increased concentration of $[K^+]$. b) Comparative complex impedance plot at dc bias of -0.20 V versus Ag/AgCl in $[Ru(NH_3)_6]^{3+}/[Ru(NH_3)_6]^{2+}$ (1 mM) in an aqueous solution of tetraethylammonium chloride (0.1M) for the monolayer **3** in presence of $[Na^+]$ and $[K^+]$ (60 mM). The frequency range used was 1 kHz to 0.1 Hz with a 5 mV rms signal at ten steps per decade. Solid lines are the fit to the experimental response by using the appropriate equivalent circuit.

Similar to the behavior exhibited by SAMs of **1** and **2**, almost no blocking of the charge-transfer process is observed (very low R_{ct} value: 0.15 kΩ) with no well-defined semicircle at the higher frequency side. But R_{ct} gradually increases from 2.6 kΩ at 5 mM to a maximum value of 18.9 kΩ at 70 mM; this indicates that there is K^+ complexation at the interface.[6] The $[K^+/Na^+]$ selectivity of this monolayer was also tested by impedance measurements. Upon addition of Na^+, the R_{ct} value increases from 1.15 kΩ at 5 mM, to a maximum of 6.23 kΩ at 45 mM of Na^+. Figure 4b shows the impedance response of the monolayer of **3** in K^+ (60 mM) and in Na^+ (60 mM). It is evident that $[Na^+]$ interacts with the monolayer to a lesser extent than $[K^+]$.

0947-6539/00/0623-4388 $ 17.50+.50/0 *Chem. Eur. J.* **2000**, *6*, No. 23

Figure 5 shows a plot of ΔR_{ct} versus concentration of $[K^+]$ and $[Na^+]$ for SAMs of **2** and **3**. The SAM of **3** showed a linear increase in R_{ct} with increased concentration of $[K^+]$; this is in

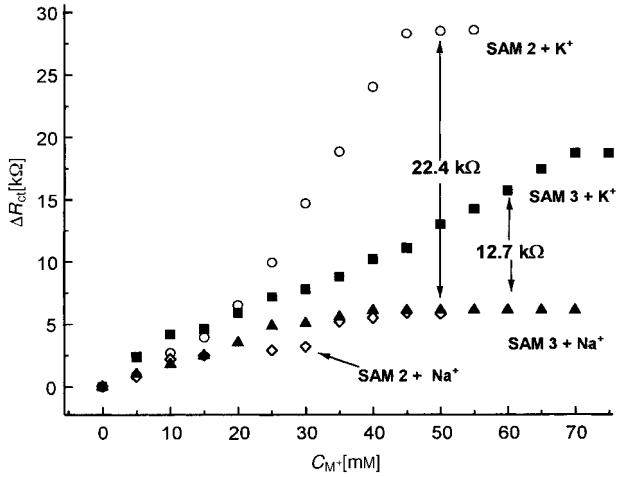

Figure 5. Comparative plot of ΔR_{ct} versus concentration of $[Na^+]$ and $[K^+]$ for monolayer **2** and **3**.

contrast to a sigmoid-type response for the SAM of **2**. The limiting R_{ct} value was reached at a comparatively lower $[K^+]$ for the monolayer of **2** ($\approx$45 mM) compared with that for **3** ($\approx$75 mM). In addition, both monolayers show essentially no response to $[Na^+]$. The difference in the limiting R_{ct} values for the monolayer of **2** in the presence of $[K^+]$ (relative to that for $[Na^+]$) is higher (22.4 kΩ) compared with that for the monolayer of **3** (12.7 kΩ); this indicates higher K^+ selectivity for **2**. Control experiments with monolayers of **4** and **5** show no ion recognition effect on the R_{ct} values. Thus the polyoxyethylene backbone as well as the two surface-binding groups at the extremes are necessary for the formation of ion recognition motifs at the surface.

As recently reported by Flink et al,[6b] our monolayers also show very small capacitance changes. So R_{ct} was the parameter of choice to follow metal ion binding. A linear change in R_{ct} with $[M^+]$ has been observed by Flink et al,[6] as well as by us for the monolayer of **3**. In contrast, as mentioned earlier, a sigmoid-type change is observed for the monolayer of both **1** and **2**. These data can be fit by using a Langmuir isotherm; this assumes that the R_{ct} parameter is a direct measure of ion binding. In Equation (1), θ corresponds to the fraction of

$$\theta = 1 - [R_M/R_c] \quad (1)$$

occupied surface-binding sites; the fraction increases with the metal ion concentration in solution. R_M and R_c correspond to the charge-transfer resistances of the monolayer alone and to the values for each metal ion concentration, respectively. So θ can be calculated from Equation (1) and can be plotted versus concentration.

For a Langmuir isotherm, θ can be related to the association constant (K_a) as in Equation (2).

$$\theta = K_a c/[1 + K_a c] \quad (2)$$

In this equation, c is the concentration of the metal ion in solution. Figure 6 shows the plots after fitting the data for **2** and **3** with K^+ to a Langmuir isotherm. K_a values of $2839 \pm 55\,M^{-1}$ and $103 \pm 8\,M^{-1}$ **3** and **2** were determined, respectively.

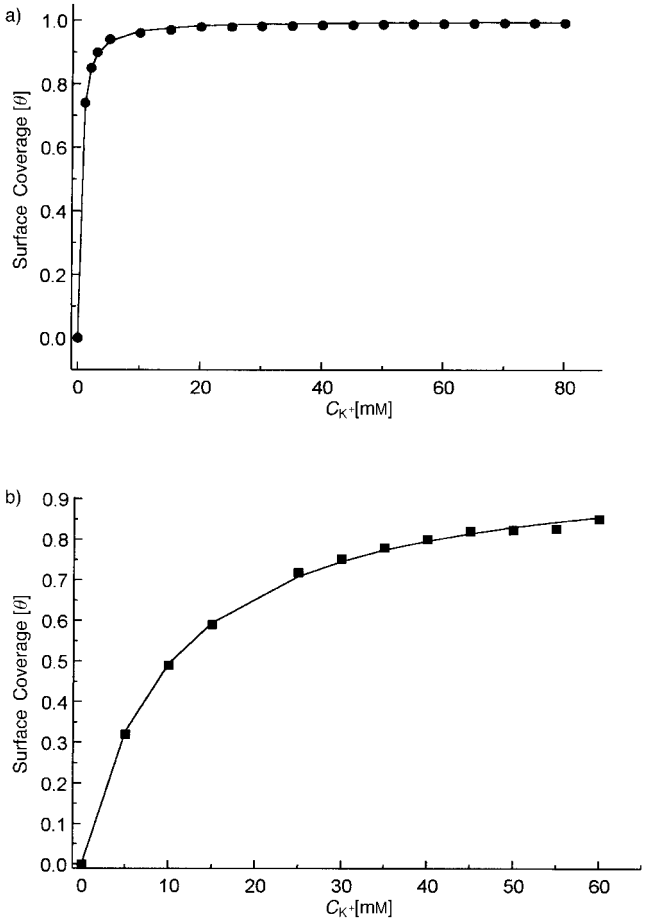

Figure 6. Plot of surface coverage, as calculated from Equation (1) versus concentration of $[K^+]$ for a) monolayer of **3** and b) monolayer of **2**. The continuous line corresponds to the fitting of respective data to the Langmuir model in order to obtain the association constant (K_a).

The association constant for monolayer **3** is an order of magnitude higher than that of **2**, as expected from the result presented in Figure 6 for the two monolayers. While a direct comparison of the binding results for **1** and **2** relative to those of **3** may not seem warranted as a result of intrinsic differences (ether vs. ester oxygens), it is instructive to do so to establish their binding preferences. Combination of Equation (1) and (2) leads to Equation (3).

$$\Delta R_{ct}/R_M = K_a c \quad (3)$$

In this equation, $\Delta R_{ct} = R_c - R_M$. Equation (3) shows a linear relation between the association constant and R_{ct} as also observed by Flink et al. and provides an alternative way to determine K_a values.[6] The calculated association constants based on Equation (3) for the different monolayers and metal ions are listed in Table 3 along with those obtained by fitting to the Langmuir isotherm. The calculated and fitted values for monolayers of **2** and **3** are within experimental error, and this

Table 3. Association constants [log K_a] of metal ions with different SAMs determined by fitting a Langmuir model and calculated from changes of charge-transfer resistance.[a]

	SAM of **1**	SAM of **2**	SAM of **3**	18-crown-6[b]	15-crown-5[b]
K^+	1.26	2.82 (2.14)	3.25 (3.45)	2.03	0.76
Na^+	1.99 (1.79)	1.42	2.95	0.9	0.67

[a] Quantities inside the brackets are association constants obtained by fitting a Langmuir model from a plot of θ versus concentration of the respective metal ion (see text). [b] In aqueous solution.

confirms the validity of the model. The association constant values are comparable with those for the corresponding crown ether–metal complexes in aqueous solution.[18] This observation is different from that of Flink et al,[6b] who measured higher values, and this suggests a lower polarity within the monolayer environment.

In contrast, the association constants obtained here suggest a similar dielectric medium within the monolayer and in the surrounding aqueous solution. These observations are in agreement with the initial characterization of the monolayers, which showed that these are loosely packed and contain holes in the structure that allow easy access of the electrolytes (also evident from the low surface coverage, higher capacitance, and from the position of the $-CH_2$ symmetric and antisymmetric stretching band in RAIR studies Tables 1 and 2). Most importantly, the monolayers of **2** and **3** show similar selectivities for K^+ over Na^+, while that of **1** shows a reverse selectivity for Na^+ over K^+. This observation suggests that during the self-assembly process at the solid/liquid interface, these podands probably form ion binding domains similar to pseudocrown ether structures, and these are capable of recognizing cations, in the same way as crown ethers, in solution or as terminal groups in a monolayer.

In order to find out the origin of the sigmoid binding curves for monolayer **1** and **2**, a Scatchard plot was prepared[18] from the data presented in Figure 7. Figure 7a shows a Scatchard plot for the monolayer **3** compared with a nonlinear plot for **1** and **2** (Figure 7b); this indicates that there is cooperative binding for podands. This behavior can be further confirmed by constructing the corresponding Hill plots,[19] which are presented in Figure 8. The Hill coefficients (n_H) determined from the slopes by linear regression were 2.1, 1.7, and 0.7 for monolayers of **1**, **2**, and **3**, respectively, and this indicates positive cooperativity in the binding process for the two podands and a noncooperative behavior for the crown-appended monolayer. The positive cooperative effect may possibly be due to the reorganization of monolayers upon ion binding.

Conclusion

Self-assembled monolayers of bis-thioctic ester podand derivatives show similar cation binding properties and higher selectivities to those of analogous crown ethers in aqueous solution. SAMs of **1**, which contains three ether oxygens and two ester groups, are selective for Na^+ over K^+, while those of **2**, with four ether oxygens and two ester groups, exhibit the

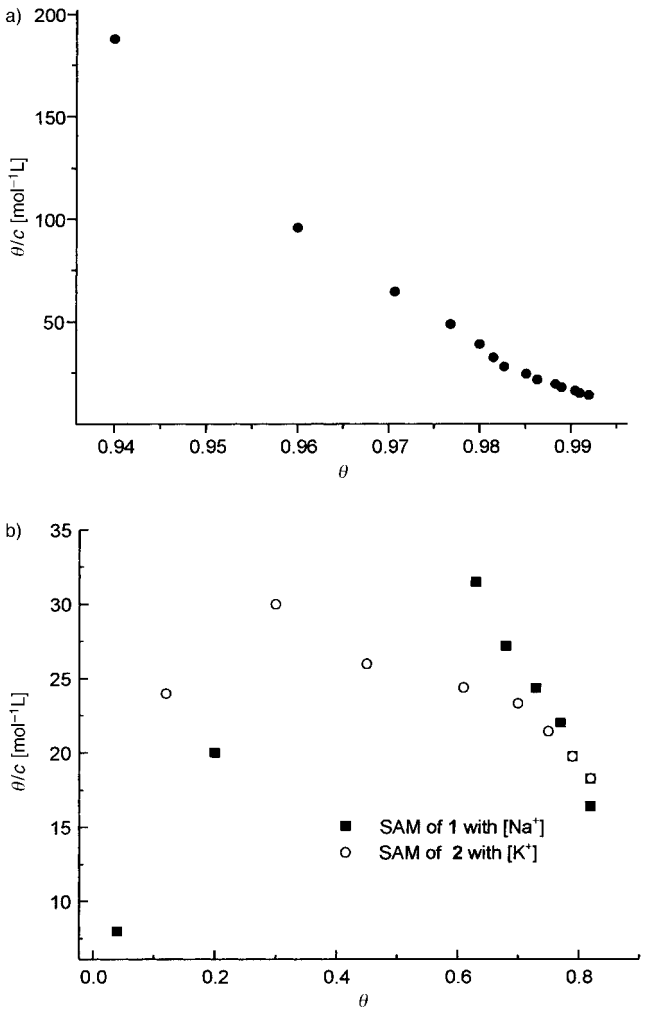

Figure 7. Scatchard plot for a) monolayer **3** with [K^+] and b) monolayer **1** and **2** with [Na^+] and [K^+], respectively.

reverse selectivity. SAMs of **3**, with an 18-crown-6 appended, are also selective for K^+ over Na^+. Application of a Langmuir isotherm model shows lower association constants for the podands than for **3**, and K^+ selectivity is higher for **2** than for **3**. Moreover, a positive cooperative effect is observed for the monolayers of the podands, but the process is noncooperative for the crown-appended monolayer. While ion sensing is a long range goal of the present work, the novelty behind this paper rests not on the preparation of better sensors but on a new concept, which uses acyclic ethylene glycol derivatives that self-assemble on gold to yield ion recognition domains.

Experimental Section

General procedure for the preparation of compounds 1–5: The corresponding alcohol (2–4 mmol) and thioctic acid (2.25 mole equiv for dialcohols or 1.1 mole equiv for monoalcohols) were added to CH_2Cl_2 (10 mL). The mixture was stirred for 15 min at 0 °C (ice/water bath) under N_2. Then, dicyclohexyl carbodiimide (DCC, 4.2 mole equiv for dialcohols or 2.1 mole equiv for monoalcohols) and 4-dimethylaminopyridine (DMAP, 0.6 mole equiv for dialcohols or 0.3 mole equiv for monoalcohols) in cold CH_2Cl_2 (10 mL) were added to the above solution, and the mixture was stirred for another 15 min at 0 °C. The cooling bath was then removed, and the solution allowed to warm to room temperature. After stirring for

0947-6539/00/0623-4390 $ 17.50+.50/0 *Chem. Eur. J.* **2000**, *6*, No. 23

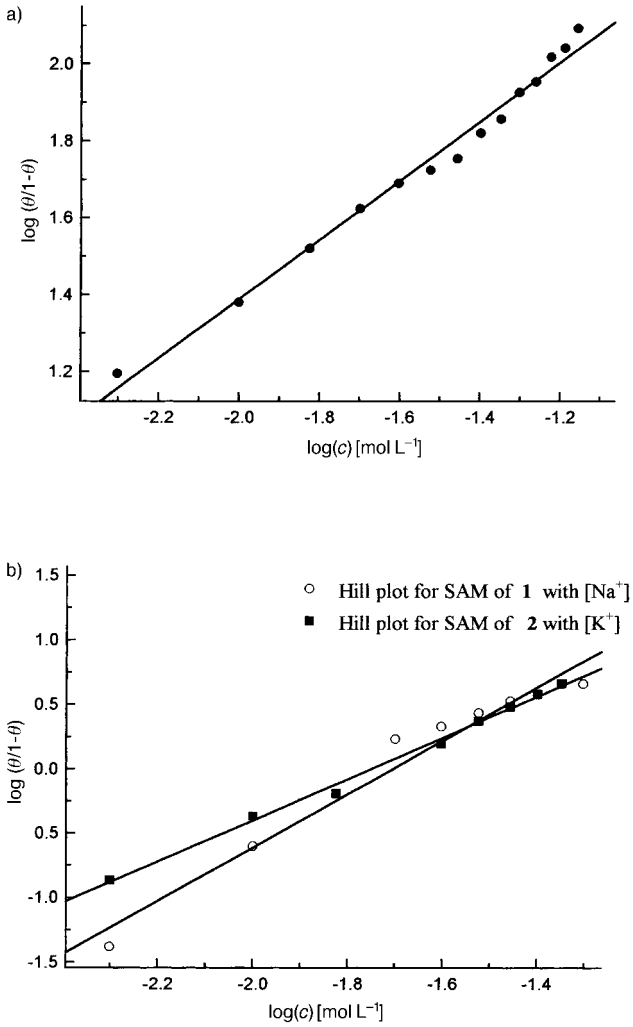

Figure 8. Hill plot for a) monolayer **3** with $[K^+]$ and b) monolayer **1** and **2** with $[Na^+]$ and $[K^+]$, respectively. The solid lines are the linear regressions of the respective data.

72 h under N_2, the reaction mixture was filtered through a fine glass frit to yield a clear, pale yellow filtrate and an insoluble urea byproduct as a fine, white gray powder. The clear filtrate was washed with water (3×50 mL), acetic acid aqueous solution (5%, 3×20 mL), and finally again with water (3×30 mL). The organic layer was dried over $MgSO_4$, filtered, evaporated, and the residue was subjected to column chromatography on silica gel (230–400 mesh).

Spectroscopic data for compounds **2**, **4**, and **5** were reported in ref. [8].

Compound 1: Eluent: ethyl acetate/CH_2Cl_2 (1:1). Pale yellow oil in 72% yield. ^{1}H NMR (300 MHz, RT, $CDCl_3$): $\delta = 1.41-1.48$ (m, 4H), 1.62–1.67 (m, 8H), 1.90–1.94 (m, 2H), 2.35 (t, $J = 7.1$ Hz, 4H), 2.45–2.48 (m, 2H), 3.11–3.19 (m, 4H), 3.55–3.59 (m, 2H), 3.66–3.70 (m, 12H), 4.31 (t, $J =$ 6.0 Hz, 4H); ^{13}C NMR (75 MHz, RT, $CDCl_3$): $\delta = 25.01, 29.04, 34.32, 34.94, 38.83, 40.57, 56.69, 63.79, 69.57, 70.97, 71.03, 173.68$; FAB$^+$-MS: m/z: 570 $[M]^+$ (80%); HRMS calcd for $C_{24}H_{42}O_7S_4$: 570.1813; found 570.1813.

Compound 3: Eluent: CH_2Cl_2/acetone (4:1). Pale yellow oil in 65% yield. ^{1}H NMR (400 MHz, RT, $CDCl_3$): $\delta = 1.36-1.42$ (m, 2H), 1.54–1.64 (m, 4H), 1.78–1.87 (m, 1H), 2.26 (t, $J = 8.0$ Hz, 2H), 2.34–2.42 (m, 1H), 3.02–3.12 (m, 2H), 3.45–3.52 (m, 1H), 3.54–3.63 (m, 20H), 3.70–3.74 (m, 3H), 4.01–4.06 (m, 1H), 4.13–4.17 (m, 1H); ^{13}C NMR (100 MHz, RT, $CDCl_3$): $\delta = 24.63, 28.71, 33.96, 34.57, 38.45, 40.19, 56.30, 63.82, 69.92, 70.71, 70.96, 71.09, 173.25$; FAB$^+$-MS: m/z: 482 $[M]^+$ (100%); HRMS calcd for $C_{21}H_{38}O_8S_2$: 482.2008; found 482.2008.

Materials: The gold substrates for the cyclic voltammetric and impedance experiments were prepared by annealing the tip of a gold wire (99.999%, 0.5 mm diameter, Alfa Ashe) in a gas-oxygen flame. Subsequently, the hot gold bead was cooled by immersion in deionized water (Barnstead Nanopure 18 MΩ). The reproducibility of the electrode surface was checked by observing the reversible redox response of $[Ru(NH_3)_6]^{3+}$/$[Ru(NH_3)_6]^{2+}$ in aqueous KCl. Electrodes that did not exhibit the reversible response of the redox couple with peak to peak separation ≈ 60 mV were discarded. The geometric area of the electrode (typically 0.02–0.04 cm^2) was obtained from the slope of a linear plot of the cathodic current versus (scan rate)$^{1/2}$ for the reversible reduction of the above mentioned redox probe; 7.5×10^{-6} cm^{2}s^{-1} was taken as the diffusion coefficient, and the exact concentration was known from the mass.[20] The gold substrates for RAIRS were prepared by vacuum deposition of gold (at a pressure of $\approx 10^{-7}$ Torr) on glass microslides coated with 3-mercaptotrimethoxysilane for better adhesion.[21]

KCl, NaCl, CsCl, $BaCl_2$, $CaCl_2$, hexammineruthenium(III) chloride, and tetraethylammoniumchloride were obtained from Aldrich and used as received.

Preparation of monolayers: In a typical experiment, a monolayer was grown by dipping a freshly-prepared gold bead electrode into a deaerated ethanolic solution (5 mM) of the respective compound for 36 hours to achieve optimum coverage. The substrates were then removed, rinsed with solvent, and dried in a stream of Ar.

Electrochemical measurements: Impedance and cyclic voltammetric measurements were performed by using a three-electrode cell with a gold bead as the working electrode, a coiled platinum wire as the counter-electrode, and an aqueous Ag/AgCl solution (from BAS) as the reference electrode. Both electrochemical experiments were carried out with a BAS 100W electrochemical workstation interfaced with a personal computer. Impedance measurements were performed at the formal potential of the redox couple, and readings were taken at ten discrete frequencies per decade. The formal redox potential $[E_{1/2} = (E_p^c + E_p^a)/2]$ was determined by cyclic voltammetry (where the concentration of $[Ru(NH_3)_6]^{3+}$ is equal to the concentration of $[Ru(NH_3)_6]^{2+}$). The frequency range utilized was 1 kHz to 0.1 Hz with an ac-amplitude of 5 mV. Impedance analysis was carried out by using the commercially available program EQUIVALENT CIRCUIT written by B. A. Boukamp (University of Twente), which determines the parameters of the assumed equivalent circuit by a nonlinear least-squares fit.[22] All experiments were carried out at room temperature ($25 \pm 0.1\,^\circ$C) with tetraethylammonium chloride (0.1M) as supporting electrolyte.

Infrared spectroscopy: The reflection-absorption infrared spectra were recorded on a Perkin-Elmer 2000 FT-IR spectrophotometer, equipped with a grazing angle (80°) infrared reflection accessory and a ZnSe wiregrid polarizer from International Crystal Laboratory. The spectra were recorded with a liquid nitrogen cooled MCT detector, and the measurement chamber was continuously purged with nitrogen gas during the measurements. Typically 1000 scans with 4 cm^{-1} resolutions were performed to get the average spectra. A clean and freshly prepared gold plate was used to record the reference spectra. The RA spectra are reported as $-\log(R/R_0)$, where R and R_0 are the reflectivities of the sample and reference, respectively.

The transmission infrared spectra of the compounds were recorded for thin films prepared by putting a drop of the solution of the compound on a quartz cell and then evaporating with a flow of Ar; the spectra were obtained by using the same spectrometer with 500 scans and 4 cm^{-1} resolution.

Acknowledgements

The authors thank the National Science Foundation for generous financial support (Grant CHE-9816503).

[1] H. O. Finklea in *Electroanalytical Chemistry, Vol. 19* (Eds.: A. J. Bard, I. Rubinstein), Marcel Dekker, New York, **1996**, p. 109.

[2] a) I. Rubinstein, S. Steinberg, Y. Tor, A. Shanzer, J. Sagiv, *Nature* **1998**, *332*, 426; b) S. Steinberg, Y. Tor, E. Sabatani, I. Rubinstein, *J. Am.*

Chem. Soc. **1991**, *113*, 5176; c) S. Steinberg, I. Rubinstein, *Langmuir* **1992**, *8*, 1183; d) L. Turyan, D. Mandler, *Anal. Chem.* **1994**, *66*, 58; e) L. Turyan, D. Mandler, *Anal. Chem.* **1997**, *66*, 1183.

[3] a) Y. Gafni, H. Weizman, J. Libman, A. Shanzer, I. Rubinstein, *Chem. Eur. J.* **1996**, *2,* 759; b) T. Stora, R. Hovious, Z. Dienes, M. Pachoud, H. Vogel, *Langmuir* **1997**, *13*, 5211; c) C. Henke, C. Steinem, A. Janshoff, G. Steffan, H. Lufthmann, M. Sieber, H.-J. Galla, *Anal. Chem.* **1996**, *68*, 3158.

[4] A. J. Moore, L. Goldenberg, M. R. Bryce, M. C. Petty, A. P. Monkman, S. N. Port, *Adv. Mater.* **1998**, *10*, 395.

[5] a) H. Liu, S.-G. Liu, L. Echegoyen, *Chem. Commun.* **1999**, 1493; b) S. G. Liu, H. Liu, K. Bandyopadhyay, Z. Gao, L. Echegoyen, *J. Org. Chem.* **2000**, *65*, 3292.

[6] a) S. Flink, B. A. Boukamp, A. van der Berg, F. C. J. M. van Veggel, D. N. Reinhoudt, *J. Am. Chem. Soc.* **1998**, *120*, 4652; b) S. Flink, F. C. J. M. van Veggel, D. N. Reinhoudt, *J. Phys. Chem B.* **1999**, *120*, 6515.

[7] a) B. Raguse, V. L. B. Braach-Maksvytis, B. A. Cornell, L. G. King, P. D. J. Osman, R. J. Pace, L. Wieczorek, *Langmuir* **1998**, *14*, 648; b) B. A. Cornell, V. L. B. Braach-Maksvytis, B. A. Cornell, L. G. King, P. D. J. Osman, B. Ragues, R. J. Pace, *Nature* **1997**, *387*, 580; c) L. M. Williams, S. D. Evans, T. M. Flynn, A. Marsh, P. F. Knowles, R. J. Bushby, N. Boden, *Langmuir* **1997**, *13*, 751, and references cited therein; d) G. B. Sigal, M. Mrksich, G. M. Whitesides, *J. Am. Chem. Soc.* **1998**, *102*, 3464; e) P. Harder, M. Grunze, R. Dahint, G. M. Whitesides, P. E. Laibinis, *J. Phys. Chem.* **1998**, *102*, 426.

[8] K. Bandyopadhyay, H. Liu, S.-G. Liu, L. Echegoyen, *Chem. Commum.* **2000**, 141.

[9] M. D. Porter, B. B. Thomas, D. L. Allara, C. E. D. Chidsey, *J. Am. Chem. Soc.* **1997**, *109*, 3559.

[10] G. Socrates, *Infrared Characteristic Group Frequencies,* Wiley, New York, **1994**.

[11] A. J. Pertsin, M. Grunze, I. A. Garbuzova, *J. Phys. Chem.* **1998**, *102*, 4918.

[12] T. Miyazawa, K. Fukushima, Y. Ideguchi, *J. Chem. Phys.* **1962**, *37*, 2764.

[13] M. L. Bruening, Y. Zhou, G. Aguilar, R. Agee, D. E. Bergbreiter, R. M. Crooks, *Langmuir* **1997**, *13*, 770.

[14] a) M. M. Walczak, D. D. Popenoe, R. S. Deinhammer, B. D. Lamp, C. Chung, M. D. Porter, *Langmuir* **1991**, *7*, 2687; b) D. E. Weissharr, B. D. Lamp, M. D. Porter, *J. Am. Chem. Soc.* **1992**, *114*, 5860.

[15] Y. Wang, A. E. Kaifer, *J. Phys. Chem. B* **1998**, *102*, 9922.

[16] J. B. Schlenoff, M. Li, H. Ly, *J. Am. Chem. Soc.* **1995**, *117*, 12528.

[17] Q. Cheng, A. Brajter-Toth, *Anal. Chem.* **1992**, *64*, 1998.

[18] R. M. Izatt, K. Pawlak, J. S. Bradshaw, R. L. Bruening, *Chem. Rev.* **1991**, *91*, 1721.

[19] D. Fitzmaurice, S. N. Rao, J. A. Preece, J. F. Stoddart, S. Wenger, N. Zaccheroni, *Angew. Chem.* **1999**, *111*, 1220; *Angew. Chem. Int. Ed.* **1999**, *38*, 1147.

[20] M. E. Gómez, J. Li, A. E. Kaifer, *Langmuir* **1991**, *7*, 1797.

[21] C. A. Goss, D. H. Charych, M. Majda, *Anal. Chem.* **1991**, *63*, 85.

[22] B. A. Boukamp, *Solid State Ionics* **1986**, *20*, 31.

Received: March 13, 2000 [F2362]

  0947-6539/00/0623-4392 $ 17.50+.50/0